  Bull. Chem. Soc. Jpn., 62, 3911—3918 (1989)

Analysis of Cyclic Voltammograms for Polypyrrole-as-Deposited Pt/poly[tris(4-vinyl-4′-methyl-2,2′-bipyridine)ruthenium(II) perchlorate] Electrodes

Kenji MURAO,* Naoki TANAKA, and Kazuhiro SUZUKI
Advanced Research Laboratory, Hitachi Ltd., Kokubunji, Tokyo 185
(Received July 29, 1989)

Oxidation waves in cyclic voltammograms (CVs) observed during repeated potential cyclings of polypyrrole-as-deposited Pt/poly-1 electrodes (poly-1: poly[tris(4-vinyl-4′-methyl-2,2′-bipyridine)ruthenium-(II) perchlorate]) in 0.1 M TBAP/acetonitrile, that lead to the bilayer (BL) electrochemistry, have been quantitatively analyzed. As the potential cycling is repeated, the CV change occurs, i.e., decrease of the peak current and positive shift of the peak potential. This is shown to be the result of logarithmic decrease in the complementary charge transfer coefficient β in the totally irreversible thin-layer (TITL) electrochemistry. k°_{TL} (standard rate constant for polypyrrole oxidation) and C°_{TL} (initial concentration of the reduced sites in polypyrrole) have been determined to be 5.50×10^{-9} cm mol^{-1} s^{-1} and 3.15×10^{-3} mol cm^{-3}, respectively, by fitting CV data to the theory of the TITL model. The subsequent onset and growth of the CV waves in the higher potential region are explained as being due to progressive partitioning of polypyrrole sites from the TITL mode to the BL mode in which polypyrrole sites are oxidized. The partition coefficient θ, defined as the ratio of polypyrrole sites oxidized in the BL mode to all the polypyrrole sites, has been found to approximately depend on the logarithm of β. In the BL mode, a linear relationship is found between peak current and peak potential. Simulation of the CV waves has been performed based on the theoretical models of TITL and BL electrochemistry, and has revealed that a model assuming separation of polypyrrole sites into the TITL and BL modes prior to each cyclic sweep explains the occurrence of the significantly separated current peaks in both modes. These results are discussed in terms of Electrochemically driven Phase Separation (ECPS), in which the decrease in β is directly related to the separation of the mixed poly-1 and polypyrrole phase.

Fabrication of microstructures with conducting polymers such as polypyrrole[1] has been the subject of recent keen interest because of both their basic importance in solid state physics[2] and potential applications.[3-7] We previously[8] reported on the successful deposition of polypyrrole onto an electrochemically active polymer film, poly-1 (poly[tris(4-vinyl-4′-methyl-2,2′-bipyridine)ruthenium(II) perchlorate]), giving an electrode expressed as Pt/poly-1/polypyrrole. Preparation of the bilayer electrodes consists of the following two steps; 1) electropolymerization of pyrrole at a Pt/poly-1 electrode, 2) repeated potential cyclings between 2+/3+ and 2+/1+ redox potentials of the $[Ru(vbpy)_3]^{2+}$ center (vbpy: 4-vinyl-4′-methyl-2,2′-bipyridine) in 0.1 M TBAP (tetrabutylammonium perchlorate)/acetonitrile (1 M=1 mol dm^{-3}). In step 1), electropolymerization of pyrrole occurs at the platinum substrate as a result of permeation of the monomer molecules throughout the poly-1 layer, as is evidenced by the CVs (cyclic voltammograms) which indicate direct charge exchange between the polypyrrole layer and the platinum substrate.[8] This means that a mixed phase of poly-1 and polypyrrole is formed in this stage. However the subsequent potential sweeps (step 2)) ultimately result in the bilayer electrochemistry in which redox reactions of polypyrrole are totally mediated by the $[Ru(vbpy)_3]^{2+}$ sites in the poly-1 layer. These electrochemical processes contrast with those employed for the preparation of bilayer electrodes based on electro-nonconducting redoxing polymers,[9] although our electrodes finally obtained through the above steps behave essentially in the same way. During step 2), a series of characteristic CV changes have been recorded as shown in Fig. 1

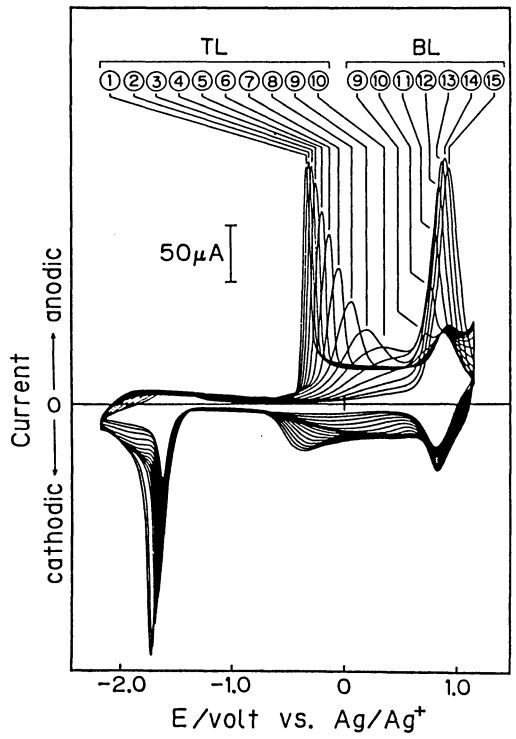

Fig. 1. Cyclic voltammograms of a polypyrrole-as-deposited Pt/poly-1 electrode measured upon repeated potential sweeps in 0.1 M TBAP/acetonitrile. Sweep rate: 0.1 V s^{-1}. (A part of this figure is reproduced from Fig. 2(b) of Ref. 8 with permission.)

(partially reproduced from Fig. 2(b) of Ref. 8). These CVs have aroused our great interest because they seem to represent certain unknown electrochemical processes that involve dynamic changes taking place in the polymer matrix. To account for the electrochemical changes, we proposed Electrochemically driven Phase Separation (ECPS) of the mixed phase from optical studies.[10] Polythiophenes have been found to undergo similar electrochemical processes.[11,12]

We show here that the CVs in Fig.1 represent a gradually developing crossover from a regime essentially described by totally irreversible thin layer electrochemistry[13] (TL regime) to bilayer electrochemistry (BL regime), associated with systematic decrease in β (complementary charge-transfer coefficient, $\equiv 1-\alpha$ where α is the charge-transfer coefficient). This finding not only supports the hypothesis of the ECPS scheme[10,14] but also provides insight into the implications of the charge-transfer coefficient in the electrochemistry of polymer-coated electrodes. The electrochemistry of polymer-coated electrodes has been studied[15-18] in relation to that of chemisorbed systems[19,20] which have the same basis as thin-layer electrochemistry.

Experimental

Materials. Preparation of the monomer precursor of poly-1, $[Ru(vbpy)_3]^{2+}$ $2PF_6^-$ was described in previous papers.[8,10] Acetonitrile was used after distillation. Commercial TBAP was purified by recrystallizing from an EtOH/H_2O 2:3 mixed solvent and was dried in vacuo at 80 °C for 32 h.

Electrochemistry. Platinum disks (3 mm diameter) embedded in glass were used as the working substrates. The surface of the platinum substrates was polished with 1 μm diamond paste. Each working electrode was sonicated three times in freshly distilled acetone, two times in trichloroethylene, two times in distilled water, and then dried at 80 °C. All of the electrochemical experiments were performed under argon-purged conditions. Electropolymerizations and electrochemical measurements were performed in a one-compartment cell with an Ag/Ag^+ quasi-reference electrode which showed 290 mV vs. SCE (saturated calomel electrode) in 0.1 M TBAP/acetonitrile. Potentials are all indicated vs. Ag/Ag^+. Deposition of poly-1 and polypyrrole were described in previous papers.[8,10] Electrochemical experiments were performed on a PAR Model 175 Universal Programmer and a 173 Potentiostat, and were recorded on a YEW 3086 X-Y Recorder.

Results and Discussion

Nature of the Cyclic Voltammograms. Figure 1 depicts the CVs for polypyrrole-as-deposited Pt/poly-1 electrode, recorded during repeated potential sweeps at a sweep rate of 0.1 V s^{-1} in 0.1 M TBAP/acetonitrile. The repeated potential sweeps lead to the bilayer electrochemistry.[8] Just after the break-in,[8] the oxidation waves of polypyrrole show sharp peaks which are not observed for Pt/polypyrrole electrodes. The following potential sweeps (**1**—**8**) cause shifts in $E_{p,TL}$ (peak potential for polypyrrole oxidation wave in the TL regime) in the positive direction associated with decrease in $i_{p,TL}$ (peak current for polypyrrole oxidation waves). In this stage, all of the polypyrrole sites are oxidized in the TL regime. Subsequently repeated potential sweeps evolve current peaks near the 2+/3+ redox potential of poly-1 (**9**,**10** in the BL regime), owing to the onset of mediated oxidation of polypyrrole, which increases with further sweeps, eventually leading to the oxidation of all polypyrrole sites in the BL mode.

To prove the nature of the sharp peaks, CVs were measured for a separate electrode (Fig. 2) in a stage approximately corresponding to **1**—**4** of Fig. 1. These CVs are anomalous in the sense that, although the sharp oxidation peak ③ is a result of direct electron transfer to the electrode, its rereduction ① is

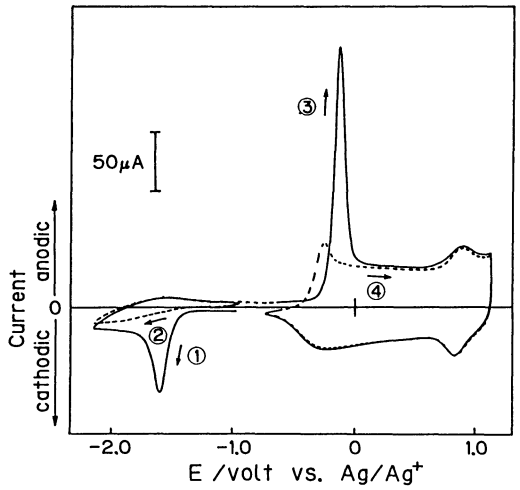

Fig. 2. Cyclic voltammograms of similarly prepared electrode as that of Fig. 1 measured in 0.1 M TBAP/acetonitrile at a sweep rate of 0.1 V s^{-1}. The CVs approximately correspond to the stage of the sweeps **1**—**4**. Numbers in circles indicate the sequence of the sweeps.

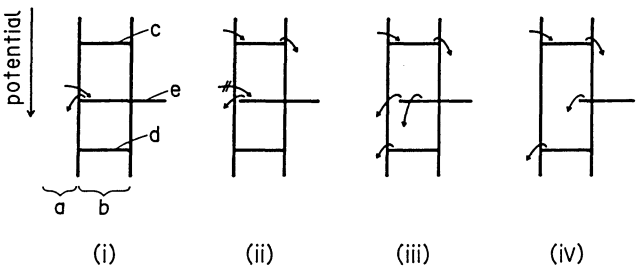

Fig. 3. Representation of possible electron transfer modes inferred on the basis of the electrochemistry depicted in Figs. 1 and 2. a: platinum electrode; b: poly-1 layer; c,d: 2+/1+ and 2+/3+ redox levels of $[Ru(vbpy)_3]^{2+}$ centers in poly-1, respectively; e: redox level of polypyrrole where the extent of phase separation is represented by relative positions of the bar.

mediated by the 2+/1+ redox level of poly-1. This implies that the sharp current peak ③ is due to the totally irreversible oxidation of polypyrrole. The nature of this peak is essentially faradaic because optical changes due to the polypyrrole oxidation are substantiated by the peak.[21]

These points are illustrated in Fig. 3. In the initial stage (i), both oxidation and reduction reactions of polypyrrole occur only through direct charge exchange with the platinum electrode. The above mentioned anomaly is shown in (ii) in which the oxidative and reductive charge transfers are effected asymmetrically. Stage (iii) corresponds to sweeps **9—12**, where both direct and indirect (mediated) oxidation modes of polypyrrole occur in a single sweep, while its rereduction is totally mediated. Stage (iv) represent the finally achieved bilayer electrochemistry corresponding to **13—15**. Hence, the electrochemistry involved in Fig. 1 can be summarized as follows; the current waves denoted by TL in Fig. 1 represent totally irreversible oxidations of polypyrrole. The following repeated potential sweeps increase the portion of polypyrrole sites that is mediatively oxidized by poly-1, eventually leading to the mediated oxidation of the whole polypyrrole sites. This suggests that the TL regime may be analyzed on the basis of the thin layer model for totally irreversible electrode processes.[13]

Analysis of Cyclic Voltammograms Using the Thin Layer Model for Totally Irreversible Electrode Processes (TITL Model). CVs for polypyrrole-as-deposited Pt/poly-1 electrodes were measured in the same way as for Fig. 1, for three separate electrodes, A—C. Coverages of poly-1 (mol cm^{-2}) and charge densities passed during the electropolymerization of pyrrole (mC cm^{-2}) are as follows, respectively; A: 3.45×10^{-9}, 40.0; B: 3.86×10^{-9}, 39.6; C: 2.68×10^{-9}, 41.2. Since the CVs involving polypyrrole include non-faradaic components significantly,[21a,b,22-24] their quantitative analysis of the whole waveforms is not straightforward. Therefore, the following analysis only considers peak currents and peak potentials which are expected to be less affected by non-faradaic contributions as mentioned above. Table 1 lists peak currents and peak potentials for electrodes A—C. Sweep number **1** for each electrode in Table 1 are determined as the sweep by which peak currents in the TL regime reach the initial saturation level after break-in.[8] Subsequent sweep numbers, as indicated in Fig. 1, are given for every consecutive three sweeps.

According to the TITL model,[13] oxidative currents upon a linear potential sweep are given by

$$i_{TL}=n_{TL}FS\,k^{\circ}_{TL}\,C^{\circ}_{TL}\exp\left\{\frac{\beta n_{o,TL}F}{RT}(E-E^{\circ}_{TL})-\frac{SRTk^{\circ}_{TL}}{\beta n_{o,TL}FVr}\exp\left[\frac{\beta n_{o,TL}F}{RT}(E-E^{\circ}_{TL})\right]\right\} \quad (1)$$

n_{TL} : number of electrons per reaction center oxidized
$n_{o,TL}$: number of electrons per reaction center oxidized in the rate-determining step
k°_{TL} : standard rate constant (cm mol^{-1} s^{-1})
C°_{TL} : initial concentration of reduced centers (mol cm^{-3})
F : Faraday constant
R : gas constant
T : absolute temperature of the reaction system
V : volume of the reaction system
S : electrode area
r : sweep rate of electrode potential (V s^{-1})
E°_{TL} : standard electrode potential

By differentiation, peak current, $i_{p,TL}$, and peak potential, $E_{p,TL}$, are obtained.

Table 1. Observed Peak Currents and Peak Potentials

Electrode	Peak No.	i_p[a]		E_p[b]	
		TL	BL	TL	BL
A	1	213		−0.340	
	2	219		−0.318	
	3	215		−0.288	
	4	199		−0.253	
	5	174		−0.200	
	6	153		−0.135	
	7	123		−0.050	
	8	92.8		0.063	
	9	67.5	64.0	0.200	0.718
	10	51.3	102	0.365	0.750
	11		155		0.790
	12		196		0.825
	13		220		0.853
	14		222		0.878
	15		213		0.913
B	1	182		−0.398	
	2	186		−0.375	
	3	187		−0.338	
	4	180		−0.300	
	5	154		−0.263	
	6	126		−0.205	
	7	101		−0.133	
	8	82.5		−0.038	
	9	69.0	60.0	0.050	0.725
	10	60.0	89.0	0.100	0.750
	11	48.5	113	0.220	0.785
	12		130		0.795
	13		151		0.810
	14		165		0.823
	15		170		0.850
C	1	237		−0.325	
	2	241		−0.313	
	3	241		−0.300	
	4	237		−0.275	
	5	227		−0.248	
	6	198		−0.210	
	7	140		−0.155	
	8	90.0		−0.045	
	9	77.0	56.3	0.380	0.733
	10	59.0	88.8	0.208	0.760
	11	47.3	141	0.375	0.800
	12		181		0.825
	13		209		0.850
	14		223		0.875
	15		221		0.905

a) 10^{-6} A. b) V vs. Ag/Ag^{+}.

$$i_{p,TL}=\frac{\beta n_{o,TL}\, n_{TL}\, F^2\, V\, r\, C^\circ_{TL}}{eRT} \quad (2)$$

$$E_{p,TL}=E^\circ_{TL}+\left(\frac{RT}{\beta n_{o,TL}\, F}\right)\ln\left(\frac{\beta n_{o,TL}\, FVr}{SRTk^\circ_{TL}}\right) \quad (3)$$

Since β values for each ($i_{p,TL}$, $E_{p,TL}$) set are not known, direct evaluation of the data in Table 1 with Eqs. 2 and 3 is not practical. By combining Eqs. 2 and 3, $\beta n_{o,TL}$ is eliminated to give

$$f(i_{p,TL})\equiv\frac{n_{TL}\, FVr\, C^\circ_{TL}}{ei_{p,TL}}\ln\frac{ei_{p,TL}}{n_{TL}\, FSC^\circ_{TL}\, k^\circ_{TL}}=(E_{p,TL}-E^\circ_{TL}) \quad (4)$$

An alternative criterion is to see if the sets ($i_{p,TL}$, $E_{p,TL}$) in Table 1 systematically fit in with Eq. 4. Since the exact values of V and C°_{TL} for polypyrrole sites are not available, the (V, k°_{TL}, C°_{TL}, E°_{TL}) set that fits the (i_{TL}, E_{TL}) data was sought. As a result, a linear fit to $f(i_{p,TL})$ vs. ($E-E^\circ_{TL}$), though only for a part in the TL regime, has been found for electrode A as shown in Fig. 4(a), when $V_A=0.636\times10^{-6}$ cm^3, $k^\circ_{TL}=5.50\times10^{-9}$ cm mol^{-1} s^{-1}, $C^\circ_{TL}=3.15\times10^{-3}$ mol cm^{-3}, $E^\circ_{TL}=-0.535$ V and $n_{TL}=n_{o,TL}=1$. Here, each peak current is assumed to include a background current of 5 μA. Owing to the fact that the E°_{TL} (or $E^{\circ\prime}_{TL}$) value cannot be pinpointed

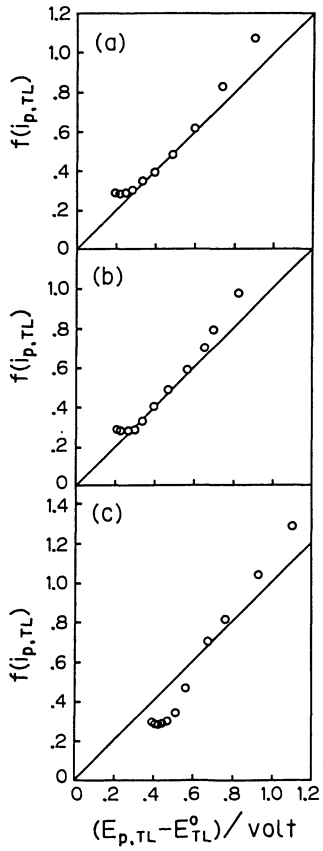

Fig. 4. Plots of $f(i_{p,TL})$ vs. ($E_{p,TL}-E^\circ_{TL}$), according to Eq. 4. $k^\circ_{TL}=5.50\times10^{-9}$ cm mol^{-1} s^{-1}, $C^\circ_{TL}=3.15\times10^{-3}$ mol cm^{-3}. E°_{TL} values: (a) −0.535 V; (b) −0.600 V; (c) −0.720 V. (a)—(c) correspond to electrodes A—C, respectively.

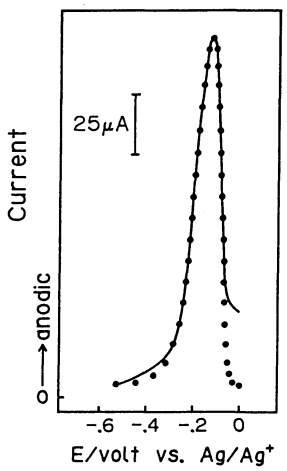

Fig. 5. Fitting of the voltammogram calculated based on Eq. 1 by using the same (V, k°_{TL}, C°_{TL}, E°_{TL}) parameters for electrode A as in Fig. 4(a) (dots). β=0.525. The solid line represents the oxidation wave of the sweep number **6** of electrode A.

in the original CV, the parameter set (V, k°_{TL}, C°_{TL}) that gives similar linearity can exist not uniquely because of the small changes in E°_{TL}. However, it has been found that current waves calculated based on Eq. 1 using the above particular parameter set fit in with the experimental waveforms, as exemplified for electrode A in Fig. 5. Here the same amount of background current, 5 μA, is assumed as in Fig. 4. This result also gives further evidence that the sharp oxidation peaks in the TL regime in Fig. 1 are essentially faradaic.

Furthermore, it has been found that, when V_B and V_C are given by 'normalization' as indicated below, ($i_{p,TL}$, $E_{p,TL}$) sets of the electrodes B and C also show linearity similar to Fig. 4 (a), as shown in Fig. 4(b) and (c), respectively, with precisely the same (k°_{TL}, C°_{TL}) set used in Fig. 4(a). This normalization is based on the $i_{p,TL}$ values of sweep number **1** of each electrode so that $V_B=V_A\times i_{p,TL}(B)/i_{p,TL}(A)$ and $V_C=V_A\times i_{p,TL}(C)/i_{p,TL}(A)$. This normalization is not unreasonable since the peak current is known to be proportional to V (or S for surface systems) in thin layer[13] and chemisorbed[19,20] systems, regardless of their electrochemical reversibility. The fact that precisely the same set of (k°_{TL}, C°_{TL}) fits the ($i_{p,TL}$, $E_{p,TL}$) sets of the separate electrodes with apparently different coverages (A, B, and C) is a strong indication that major portions of the data in Table 1 can be described essentially by the TITL model. Different E°_{TL} values are obtained for the three electrodes by the fitting procedure, i.e., A: −0.535 V; B: −0.600 V; C: −0.720 V. Such differences persist even when different (k°_{TL}, C°_{TL}, E°_{TL}) sets, that give the similar linearity, are used. Since the deviations of the plots from the linearity are larger in Fig. 4(c) than in the other two cases, E°_{TL} values of electrodes A and B seem to be more reliable. In fact, the E°_{TL} values for electrodes A and B are only slightly different from $E^{\circ\prime}$ values of

polypyrrole estimated on the basis of the separations of E_{pa} and E_{pc}.[25,26]

Significant deviations from the linearity are seen in Fig. 4 for both smaller and larger sweep numbers. Although the electrochemical mechanism that governs the initial sweeps is not known, it may be due to some strong interactions between polypyrrole and the electrode substrate. The deviations in larger sweep numbers ($\geq$8), in which BL mode oxidation also occurs, are understood as a result of the reductions in $i_{p,TL}$ due to partial consumption (oxidation) of C°_{TL} in the BL mode. This partitioning of C°_{TL} from the TL to BL mode is further analyzed in the following sections.

Estimation of Complementary Charge Transfer Coefficient. In plotting Fig. 4, all parameters in Eq. 4 are fixed except for β. Hence, the different values of $f(i_{p,TL})$ are assumed to be generated by the changes in β values in Eqs. 2 and 3 for each cyclic sweep. Thus the β values can be obtained from these equations. However, it should be noted that, because of the partitioning of C°_{TL} from the TL to BL modes for sweep numbers larger than **8** as mentioned above, β values obtained from Eq. 2 can be inaccurate. Therefore, β is alternatively estimated, by using experimental $E_{p,TL}$ values and the parameter set used in Fig. 4, based on Eq. 3 in which β is not dependent on C°_{TL}. The result of the calculations are shown in Fig. 6. It is seen from Fig. 6 that β values decrease logarithmically as the sweep number increases, meeting the condition of $0 \leq \beta \leq 1$ for $E_{p,TL}$ values that fit linearly in with Fig. 4. On the other hand, β values obtained for $E_{p,TL}$ values from ($i_{p,TL}$, $E_{p,TL}$) sets, that deviate significantly from the linearity in Fig. 4, deviate from the linearity and/or violate the $\beta \leq 1$ condition.

If one gets 'intact' $i_{p,TL}$ values without TL$\rightarrow$BL partitioning ($i^{\circ}_{p,TL}$) from Eq. 2, by using β values in Fig. 6 and the same (V, C°_{TL}) set in Fig. 4, then one should be able to estimate the deviation of the experimental $i_{p,TL}$ values from the corresponding $i^{\circ}_{p,TL}$. Such calculations for electrodes A—C have shown that the deviation defined by $\delta \equiv (i^{\circ}_{p,TL} - i_{p,TL})/i^{\circ}_{p,TL}$ increases approximately linearly as the sweep number increases from **8** (Fig. 7(a)). δ should be directly related to the partition coefficient θ (defined as the ratio of polypyrrole sites oxidized in the BL mode to all the polypyrrole sites), since $i_{p,TL}$ is proportional to C°_{TL} (Eq. 2). Estimation of δ (and hence θ) as above is possible only for sweep numbers smaller than **12**, because well defined current peaks are detectable only for them. Since $\ln\beta$ is approximately proportional to sweep number (Fig. 6), the results in Fig. 7(a) suggest that δ may be proportional to $\ln\beta$. δ vs. $\ln\beta$ plots in Fig. 7(b) confirms such expectation, where both values are roughly proportional each other. The result in Fig. 7(b) implies that the progress of the crossover, and hence the phase separation of poly-1 and polypyrrole,

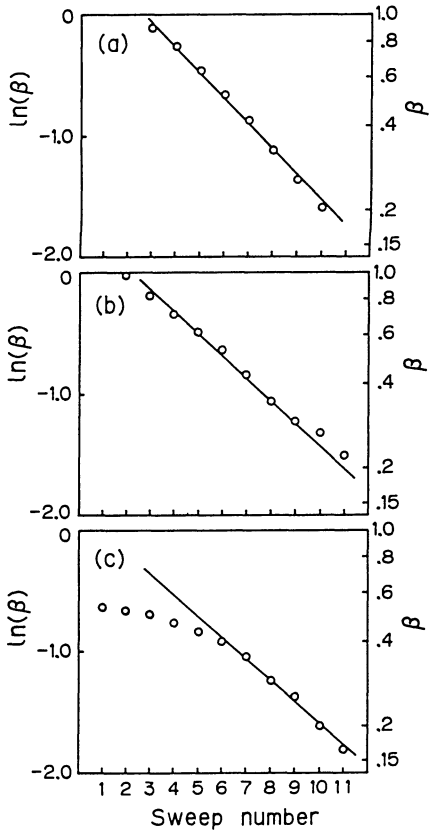

Fig. 6. Plots of ln β vs. the sweep number. β values were obtained based on Eq. 3 using the same parameters as in Fig. 4. β values exceeding unity are neglected. (a)—(c) correspond to electrodes A—C, respectively.

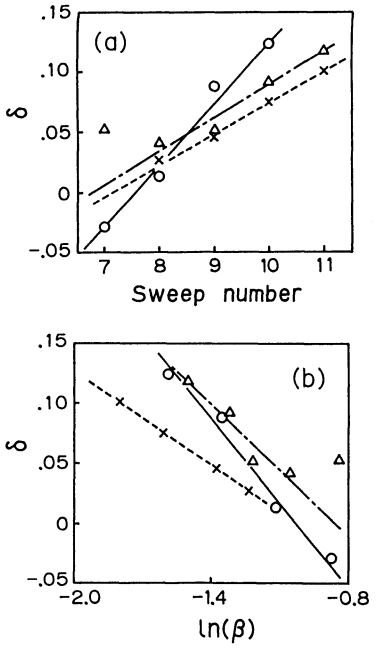

Fig. 7. (a): plot of δ vs. sweep number I; (b): plot of δ vs. ln β (β: complementary charge transfer coefficient). $\delta \equiv (i^{\circ}_{p,TL} - i_{p,TL})/i^{\circ}_{p,TL}$. —○—, —·—△—·—, and ···×··· represent electrode A, B, and C, respectively.

may be expressed as a function of β.

Analysis of the Mediated Oxidation Waves of Polypyrrole (BL Regime). A linear relationship has been found between the peak currents in the BL regime, $i_{p,BL}$, and the peak potentials ($E_{p,BL}-E^{\circ\prime}_{BL}$) ($E^{\circ\prime}_{BL}$: formal oxidation potential of $[Ru(vbpy)_3]^{2+}$ centers of the inner layer, +0.85 V), as shown in Fig. 8, although contributions by the inner layer are neglected here.

A theoretical treatment of bilayer electrochemistry[9b,27] has been presented for a case in which the e^- transfer process across the interface is the rate-determining step and a Nernstian equilibrium is established throughout the inner layer except for the interface layer.

$$i_{BL}=n_{ch,BL}\,FS\,k^{\circ}_{BL}\,\phi^2\{1+\exp[f(E_{init}-E^{\circ\prime}_{BL})]\}^{p}\times\{1+\exp[f(E_{init}+rt-E^{\circ\prime}_{BL})]\}^{-p-1}\times\exp[f(E_{init}+rt-E^{\circ\prime}_{BL})] \quad (5)$$

where

$$p=\frac{k^{\circ}_{BL}\phi^2}{\Gamma^{\circ}_{BL}\,fr},\quad f=\frac{n_{BL}\,F}{RT}$$

$n_{ch,BL}$: number of electrons per reaction center oxidized on e^- transfer across the inner layer/outer layer interface

n_{BL}: number of electrons per reaction center oxidized

k°_{BL}: rate constant for e^- transfer across the interface ($cm^2\,mol^{-1}\,s^{-1}$)

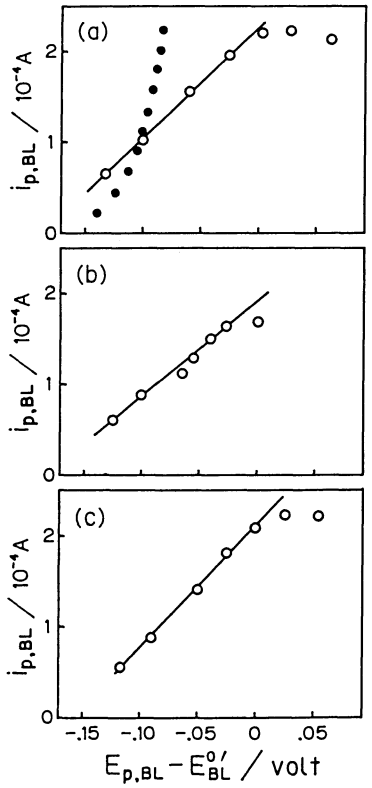

Fig. 8. Plots of $i_{p,BL}$ vs. ($E_{p,BL}-E^{\circ\prime}_{BL}$). Closed circles represent calculated values based on Eqs. 6 and 7. (a)—(c) correspond to electrodes A—C, respectively.

ϕ: coverage that can participate in direct charge transfer across the interface (mol cm^{-2})

E_{init}: potential at which positive potential sweep is initiated

$i_{p,BL}$ for $E_{init}\ll E^{\circ\prime}_{BL}$ are given by differentiating Eq. 5',

$$i_{p,BL}=\frac{n_{BL}\,n_{ch,BL}\,F^2\,S\,r\,\Gamma^{\circ}_{BL}}{RT}\left(1+\frac{1}{p}\right)^{-p-1} \quad (6)$$

$$E_{p,BL}=E^{\circ\prime}_{BL}-\frac{1}{f}\ln p \quad (7)$$

Closed circles in Fig. 8 represent the calculated [$i_{p,BL}$, ($E_{p,BL}-E^{\circ\prime}_{BL}$)] values based on Eqs. 6 and 7, which show no linear relationship. This would imply that assumptions employed in deriving Eqs. 5—7 are not valid in the present case. Inappropriateness of the assumptions have been noted.[27] Plots in Fig. 8 imply how $i_{p,BL}$ and $E_{p,BL}$ change when the coverage of the outer layer (number of polypyrrole sites) is variously changed as a result of increasing partitioning. $i_{p,BL}$ is also found to linearly depends on sweep number. This means that $i_{p,BL}$ and $E_{p,BL}$ may be proportional to C_{BL} or Γ_{BL}, since δ is also approximately proportional to sweep number.[28] These results povide a guideline in obtaining the analytical equations to describe the electrochemistry of the BL mode.[29]

Simulation of Cyclic Voltammograms. Simulation of the CVs in Fig. 1 has been studied on the basis of TITL model accompanying subsequent crossover to the BL mode. The following simulation is based on the assumption that portions of polypyrrole sites contributing to TL and BL mode oxidations are given separately at the beginning of each cyclic sweep (separation model). The change in β upon repeated potential sweeps is formulated according to the result of Fig. 6.

$$\beta=\exp[-0.2\times(I-1)] \qquad I\text{: sweep number} \quad (8)$$

Partition coefficient θ for each sweep is given arbitrarily, since it cannot be known for larger sweep numbers ($12\leq I$). For $12\leq I$, the BL mode oxidation prevails and no current peaks in the TL regime are detectable. Since we have not found analytical formulations that successfully describe the electrochemistry of the BL mode where charge transfer processes within both layers are considered as rate-limiting steps,[27] Eq. 5 is alternatively used to show overall waveforms at the expense of the detailed waveforms in the BL mode. The result is shown in Fig. 9. In spite of such limitations, the waveforms simulate the overall changes including the crossover phenomenon.

An alternative model on the progress of the crossover is possible as follows. The partitioning from TL to BL progresses competitively as a function of the applied potential (parallel progress model or PP model), instead of initial separation of polypyrrole sites into two distinct portions. In the PP model,

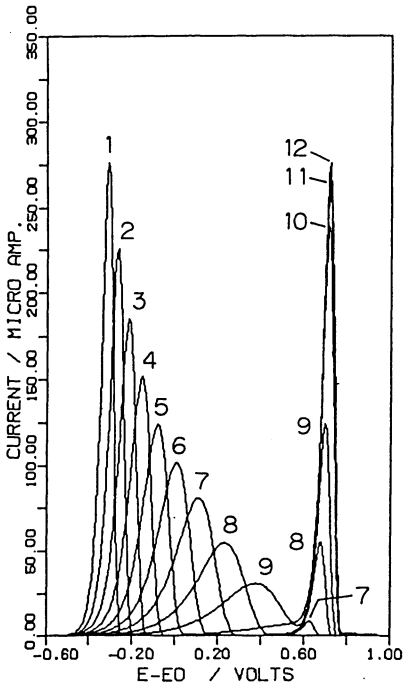

Fig. 9. Cyclic voltammograms generated based on Eqs. 1, 5, and 8, according to the separation model. E°_{TL}=−0.535 V; $E^{\circ\prime}_{BL}$=+0.850 V; E_{init}=−0.6 V. The same k°_{TL} (5.50×10^{-9} cm mol^{-1} s^{-1}) and C°_{TL} (3.15×10^{-3} mol cm^{-3}) values are used as in Fig. 4. $n_{TL}=n_{o,TL}=n_{ch,BL}=n_{BL}=1$; $k^{\circ}_{BL}=8.00\times10^{15}$ cm^2 mol^{-1} s^{-1}; $\phi=0.483\times10^{-10}$ mol cm^{-2}. Partition coefficient θ is given as; sweep number I=1—6: 0; I=7: 0.03; I=8: 0.2; I=9: 0.45; I=10: 0.86; I=11: 0.96; I=12: 1.0. β is changed from unity to 0.11.

oxidation of reduced polypyrrole sites proceeds in both modes competitively, according to the different potential dependencies defined by Eqs. 1 and 5. Simulations based on the PP model, however, have proved that this model fails to produce large current peak separations like sweep **9** of Fig. 1 in TL and BL modes in a single sweep. This model also does not produce any deviation of $i_{p,TL}$ from $i^{\circ}_{p,TL}$.

To account for the substantial change in the β value, the following explanation may be possible. The charge carriers in the oxidized state of polypyrrole are bipolarons.[2] The generation and rereduction of bipolarons in polypyrrole occur at different levels, i.e., at valence band edge and at bipolaron level, respectively. Because of this situation, polypyrrole present in the polymer matrix (poly-1) may be subject to such assymetric electrochemistry as in Fig. 2. On the other hand, the progress of phase separation of polypyrrole and poly-1 should change the distance to be moved in the reaction coordinate to achieve the oxidation of polypyrrole. This change in the distance in the reaction coordinate, associated with the above assymetry, would change β significantly.

It should be stressed that the consideration of a simple voltage-loss process in the polypyrrole oxidation cannot explain the systematic changes of the CVs in Fig. 1.

To our knowledge, there has been little preceding work on the relevance of spatial factors in polymer-coated electrodes to the charge transfer coefficient. Essentially the same CV changes have been recorded for poly(3-methylthiophene)- and poly(2,2′-bithiophene)-as-deposited Pt/poly-1 electrodes.[11] If examples of ECPS are found for other redoxing polymers without a capacitive effect, more detailed analyses will be possible, because they would provide precise experimental information on the concentration, electrochemical coverage of reaction centers, $E^{\circ\prime}$ and i_{TL} values. The ECPS scheme may find applications as means for fabricating microstructures using electroactive polymers.

Conclusion

CV changes observed during the electrochemical potential sweeps of polypyrrole-as-deposited Pt/poly-1 electrodes have been found to be essentially described by a thin layer model for totally irreversible electrode processes (TITL model) with a subsequent gradual crossover to bilayer electrochemistry (BL model). Systematic shifts of peak potential associated with the decrease in peak current in the TL mode are ascribed to the result of logarithmic decrease of the complementary charge transfer coefficient β as the sweep number increases. After each cyclic sweep of potential, the system is reset to the initial state, except that smaller β values are given after each cycle. It has been found that the model, which assumes that reduced polypyrrole sites are separated into portions of TL and BL mode oxidations prior to each cyclic potential sweep, well simulate the CV changes of Fig. 1.

The present results shed light on the electrochemical aspect of polymer phase separation. We assume that the decrease in the β value in the present study should be related to the progress of the polymer phase separation.

References

1) a) A. F. Diaz, K. K. Kanazawa, and G. P. Gardini, *J. Chem. Soc., Chem. Commun.*, **1979**, 635; b) K. K. Kanazawa, A. F. Diaz, B. H. Geiss, W. D. Gill, J. F. Kwak, J. A. Logan, J. F. Rabolt, and G. B. Street, *ibid.*, **1979**, 854; c) A. F. Diaz and J. I. Castillo, *ibid.*, **1980**, 397.

2) See for example; A. J. Heeger, *Philos. Trans. R. Soc. London, Ser. A*, **314**, 17 (1985).

3) R. A. Bull, F.-R. Fan, and A. J. Bard, *J. Electrochem. Soc.*, **130**, 1636 (1983).

4) a) H. S. White, G. P. Kittlesen, and M. S. Wrighton, *J. Am. Chem. Soc.*, **106**, 5375 (1984); b) G. P. Kittlesen, H. S. White, and M. S. Wrighton, *ibid.*, **106**, 7389 (1984); c) C.-F. Shu and M. S. Wrighton, *J. Phys. Chem.*, **92**, 5221 (1988).

5) a) P. Burgmayer and R. W. Murray, *J. Am. Chem. Soc.*, **104**, 6139 (1982); b) P. Burgmayer and R. W. Murray, *J.*

Electroanal. Chem., **147**, 339 (1983).
6) T. Skotheim and I. Lundström, *J. Electrochem. Soc.*, **129**, 894 (1982).
7) H. Koezuka and S. Etoh, *J. Appl. Phys.*, **54**, 2511 (1983).
8) K. Murao and K. Suzuki, *J. Chem. Soc., Chem. Commun.*, **1984**, 238.
9) a) H. D. Abruna, P. Denisevich, M. Umana, T. J. Meyer, and R. W. Murray, *J. Am. Chem. Soc.*, **103**, 1 (1981); b) P. Denisevich, K. W. Willman, and R. W. Murray, *ibid.*, **103**, 4727 (1981); c) K. W. Willman and R. W. Murray, *J. Electroanal. Chem.*, **133**, 211 (1982); d) C. R. Leidner, P. Denisevich, K. W. Willman, and R. W. Murray, *ibid.*, **164**, 63 (1984); e) C. R. Leidner and R. W. Murray, *J. Am. Chem. Soc.*, **107**, 551 (1985).
10) K. Murao and K. Suzuki, *J. Electrochem. Soc.*, **135**, 1415 (1988).
11) a) K. Murao and K. Suzuki, *Chem. Lett.*, **1986**, 2101; b) K. Murao and K. Suzuki, *Bull. Chem. Soc. Jpn.*, **60**, 2809 (1987).
12) K. Murao and K. Suzuki, *Solid State Commun.*, **62**, 483 (1987).
13) a) A. T. Hubbard, *J. Electroanal. Chem.*, **22**, 165 (1969); b) A. J. Bard and L. R. Faulkner, "Electrochemical Methods: Fundamentals and Applications," Wiley, New York (1980), pp. 406—413.
14) K. Murao and K. Suzuki, *Appl. Phys. Lett.*, **47**, 724 (1985).
15) a) M. S. Wrighton, R. G. Austin, A. B. Bocarsly, J. M. Bolts, O. Haas, K. D. Legg, L. Nadjo, and M. C. Palazzotto, *J. Electroanal. Chem.*, **87**, 429 (1978); b) M. S. Wrighton, M. C. Palazzotto, A. B. Bocarsly, J. M. Bolts, A. B. Fischer, and L. Nadjo, *J. Am. Chem. Soc.*, **100**, 7264 (1978).
16) a) K. Itaya and A. J. Bard, *Anal. Chem.*, **50**, 1487 (1978); b) A. Merz and A. J. Bard, *J. Am. Chem. Soc.*, **100**, 3222 (1978).
17) a) J. C. Lennox and R. W. Murray, *J. Electroanal. Chem.*, **78**, 395 (1977); b) K. Kuo, P. R. Moses, J. R. Lenhard, D. C. Green, and R. W. Murray, *Anal. Chem.*, **51**, 745 (1979).
18) a) N. Oyama, K. B. Yap, and F. C. Anson, *J. Electroanal. Chem.*, **100**, 233 (1979); b) N. Oyama and F. C. Anson, *J. Electrochem. Soc.*, **127**, 640 (1980); c) K. Shigehara, N. Oyama, and F. C. Anson, *J. Am. Chem. Soc.*, **103**, 2552 (1981).
19) a) E. Laviron, *J. Electroanal. Chem.*, **39**, 1 (1972); b) E. Laviron, *ibid.*, **100**, 263 (1979).
20) R. F. Lane and A. T. Hubbard, *J. Phys. Chem.*, **77**, 1401 (1973).
21) We note close similarity of the waveform to that of the faradaic component; a) J. Tanguy, N. Mermilliod, and M. Hoclet, *Synth. Metals*, **18**, 7 (1987); b) J. Tanguy, N. Mermilliod, and M. Hoclet, *J. Electrochem. Soc.*, **134**, 795 (1987).
22) S. W. Feldberg, *J. Am. Chem. Soc.*, **106**, 4671 (1984).
23) R. A. Bull, F.-R. Fan, and A. J. Bard, *J. Electrochem. Soc.*, **129**, 1009 (1982).
24) S. Kuwabata, H. Yoneyama, and H. Tamura, *Bull. Chem. Soc. Jpn.*, **57**, 2247 (1984).
25) A. F. Diaz, J. I. Castillo, J. A. Logan, and W.-Y. Lee, *J. Electroanal. Chem.*, **129**, 115 (1981).
26) P. G. Pickup and R. A. Osteryoung, *J. Am. Chem. Soc.*, **106**, 2294 (1984).
27) P. G. Pickup, C. R. Leidner, P. Denisevich, and R. W. Murray, *J. Electroanal. Chem.*, **164**, 39 (1984).
28) Since the slope for the plot of δ vs. I (sweep number) in Fig. 7(a) is only about 0.04, extrapolation to sweep number **14** does not yield the 100% crossover. Hence the linearity between δ and I may be established only for small I values.
29) Interestingly, we have observed similar non-linear $i_{p,TL}$ vs. $E_{p,TL}$ relationship as the closed circles of Fig. 8 for Pt/poly-1/polypyrrole electrodes with very small coverages of the inner layer ($\leqq 1.6\times10^{-9}$ mol cm^{-2}). This is probably due to the significantly reduced rate-limiting character of the inner layer.